



Shahrood University of  
Technology



Iranian Society of  
Mining Engineering  
(IRSM)

## Block Toppling Stability of Rock Block with Rounded Edges using Sarma Approach

Hassan Sarfaraz\*, Mohadesch Sarlak, Fatemeh Ashoor, and Erfan Amini

School of Mining Engineering, College of Engineering, University of Tehran, Iran

### Article Info

Received 23 January 2023  
Received in Revised form 28  
February 2023  
Accepted 3 March 2023  
Published online 3 March 2023

[DOI:10.22044/jme.2023.12630.2295](https://doi.org/10.22044/jme.2023.12630.2295)

### Keywords

Rock Slopes  
Block Toppling  
Theoretical Approach  
Sarma Methodology  
Limit Equilibrium

### Abstract

In rock slopes, block toppling failure is a prevalent instability. In this instability, rock mass consists of a series of dominant parallel discontinuities that are dipping steeply into the slope face, and a series of cross-joints are located normal to the dominant discontinuities. Blocks may slide or rotate due to their weight along the natural cross-joints at their base, and the tensile strength does not significantly affect the stability of the rock slope. The rounding edge of rock columns is a special feature of spheroidal weathering. Firstly, a literature review of block toppling instability is presented. Next, applying the Sarma approach, a new theoretical analysis is proposed for the rock columns with rounded edges. One of the advantages of the proposed approach is that by determining the sign of a parameter called KC, the stability status can be specified. The suggested solution is compared with a pre-existing analytical method through examples and case study. Comparisons indicate that the proposed approach has a satisfactory agreement. It can be concluded that with weathering and rounding of the block edges, the safety factor decreases non-linearly. Therefore, this solution can be used to evaluate the blocky toppling failure regarding the erosion phenomenon.

### Nomenclature list

$h$	Average block length	$N_i$	Normal force acting at block base
$t$	Block thickness	$S_i$	Shear force acting at block base
$\psi_f$	Slope angle	$\ell_i$	Point application of $N_i$
$\psi_p$	Joint dip inclination	$d_i$	Length of block sides
$\psi_b$	Dip of normal joints	$b_i$	Horizontal distance of block base
$\alpha_i$	Angle of block base with respect to the horizontal-axis	$\phi_b$	Interface friction angle of block base
$\delta_i$	Inclination of interface measured from the vertical-axis	$c_b$	Cohesive strength of block base
$H$	Height of slope	$c_c$	Cohesive strength on sides of blocks
$Q$	Shear force of inter-block	$\phi_c$	Interface friction angle among blocks
$y$	Point application of the normal force	$P$	Normal force of inter-block

## 1. Introduction

Toppling is a type of failure slope cut in rock masses with regularly spaced layers of foliation, and conventional instability in rock slopes is a toppling failure. Müller [1] mentioned the sliding Vaiont dam as a toppling failure. In 1970, Erguvanli and Goodman [2] conducted physical tests to examine toppling failure using a base friction device. Based on the laboratory models and theoretical methods, Ashby [3] studied rock block rotation. This researcher suggested the nomination of “toppling”. Toppling failures were categorized into primary and secondary [4]. For the primary kind of toppling failures, the rock column weight is the governing factor of the instability. Secondary toppling failures are triggered by some external factors, and there are several types of this instability [5-8].

Aydan and Kawamoto [9, 10] simulated the toppling instability through physical modeling. Toppling instabilities have been numerically modeled by the FEM and DEM softwares [11, 12]. The main kind of toppling such as flexural and block-flexural toppling failures have been analytically analyzed [13-17]. Bowa and Xia [18]

investigated the effect of the counter-tilted slip surface angle on the block toppling instability, and these researchers verified their obtained results with 3D numerical modeling. Sarfraz and Amini [19] simulated the block-flexural toppling instability via the UDEC software as a distinct element method. They concluded that the distinct element method was a suitable tool for analyzing this type of failure. Zheng *et al.* [20] presented a step-by-step analysis model to compute the safety factor related to the aforementioned failure. Zheng *et al.* [21] combined the force-transfer model with a genetic algorithm for predicting the safety factor and failure plane of a rock slope, in which the application of numerical modeling and metaheuristic methods has been investigated in various studies [22-27].

All of the above studies are to analyze the stability of toppling failure in the case of sharp block edges. Spheroidal weathering transforms the original sharp-edged prismatic blocks into blocks with rounded edges. If the weathering process continues indefinitely, spherical blocks are formed, which is shown in Figure 1.



Figure 1. Spheroidal weathering of blocks [28].

Alejano *et al.* [28, 29] studied the stability analysis of block toppling instability of rounded blocks using physical and theoretical approaches. Sarfraz [17] proposed a theoretical analysis of block-flexure toppling instability regarding the erosion effect.

In this research work, applying the Sarma methodology, a new theoretical approach was

suggested for the stability analysis of block toppling failure of blocks having rounded edges. Firstly, the Sarma approach was reviewed. Furthermore, the safety factor was obtained to analyze the stability, in which the status of the slope stability was determined by the coefficient of fictitious horizontal acceleration, and then the outcomes were discussed.

### 2. A Review of Sarma's Approach

The Sarma approach is a method of the limit equilibrium technique, which is used to determine

the slope stability. The geometry of the sliding mass is defined by the corner coordinates of the blocks and the force acting on the slice (Figure 2).

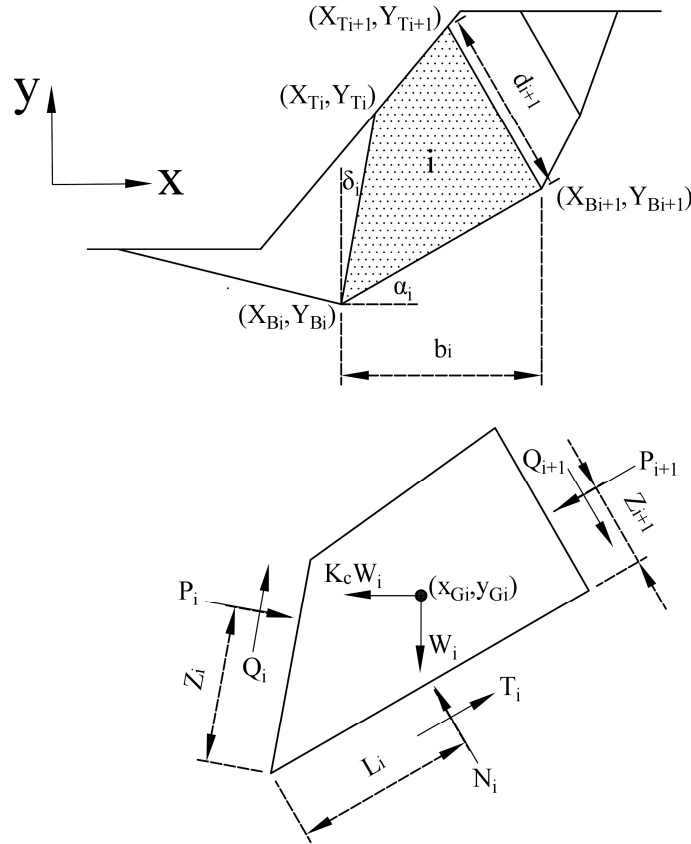


Figure 2. Definition of geometry and acting of forces.

The fictitious horizontal acceleration ( $K_C$ ) as a principle of slope stability was presented by Sarma [30]. Stability was determined via  $K_C$ . The slope is stable when this parameter is positive; the slope is the equilibrium threshold when this parameter is

zero, and the slope is unstable when this parameter is negative.

Based on Figure 2, the forces equilibrium equation in the x and y directions can be written:

$$T_i \cos \alpha_i - N_i \sin \alpha_i = K_C W_i + Q_{i+1} \sin \delta_{i+1} - Q_i \sin \delta_i + P_{i+1} \cos \delta_{i+1} - P_i \cos \delta_i \tag{1}$$

$$T_i \sin \alpha_i + N_i \cos \alpha_i = W_i + Q_{i+1} \cos \delta_{i+1} - Q_i \cos \delta_i - P_{i+1} \sin \delta_{i+1} + P_i \sin \delta_i \tag{2}$$

By applying the Mohr-Coulomb criterion to the base and the interface of the blocks, the following equations can be achieved:

$$T_i = N_i \tan \varphi_{b,i} + C_{b,i} b_i / \cos \alpha_i \tag{3}$$

$$Q_i = P_i \tan \varphi_{c,i} + C_{c,i} d_i \tag{4}$$

$$Q_{i+1} = P_{i+1} \tan \varphi_{c,i+1} + C_{c,i+1} d_{i+1} \tag{5}$$

By replacing Equations (3-5) in equations (1-2):

$$P_{i+1} = a_i + b_i P_i - c_i K_C \tag{6}$$

When there are no external forces ( $P_{i+1} = P_i = 0$ ),  $K_C$  is obtained as follows:

$$K_C = \frac{a_n + a_{n-1} b_n + a_{n-2} b_n b_{n-1} + \dots + a_1 b_n b_{n-1} \dots b_3 b_2}{c_n + c_{n-1} b_n + c_{n-2} b_n b_{n-1} + \dots + c_1 b_n b_{n-1} \dots b_3 b_2} \tag{7}$$

where:

$$a_i = \frac{\left[ \begin{aligned} &W_i \sin(\varphi_{b,i} - \alpha_i) + C_{b,i} b_i \sec \alpha_i \cos \varphi_{b,i} + C_{c,i+1} d_{i+1} \sin(\varphi_{b,i} - \alpha_i - \delta_{i+1}) \\ &- C_{c,i} d_i \sin(\varphi_{b,i} - \alpha_i - \delta_i) \end{aligned} \right] \cos \varphi_{c,i+1}}{\cos(\varphi_{b,i} - \alpha_i + \varphi_{c,i+1} - \delta_{i+1})} \quad (8)$$

$$b_i = \frac{\cos(\varphi_{b,i} - \alpha_i + \varphi_{c,i} - \delta_i) \cos \varphi_{c,i+1}}{\cos(\varphi_{b,i} - \alpha_i + \varphi_{c,i+1} - \delta_{i+1}) \cos \varphi_{c,i}} \quad (9)$$

$$c_i = \frac{W_i \cos(\varphi_{b,i} - \alpha_i) \cos \varphi_{c,i+1}}{\cos(\varphi_{b,i} - \alpha_i + \varphi_{c,i+1} - \delta_{i+1})} \quad (10)$$

The safety factor can be computed with decreasing shear strength values (C and  $\tan \varphi$  to  $C / F_S$  and  $\tan \varphi / F_S$ ) until  $K_C$  reaches zero.

### 3. Theoretical Analysis

A schematic representation of the suggested theoretical approach for rock slope with the prone of block toppling failure with round edges is shown in Figure 3, in which the geometry and forces acting on the (i+1)<sup>th</sup> block are defined in this figure. With writing the limit equilibrium conditions and Mohr-Coulomb failure criteria on the block sides, the following equations can be defined for every block:

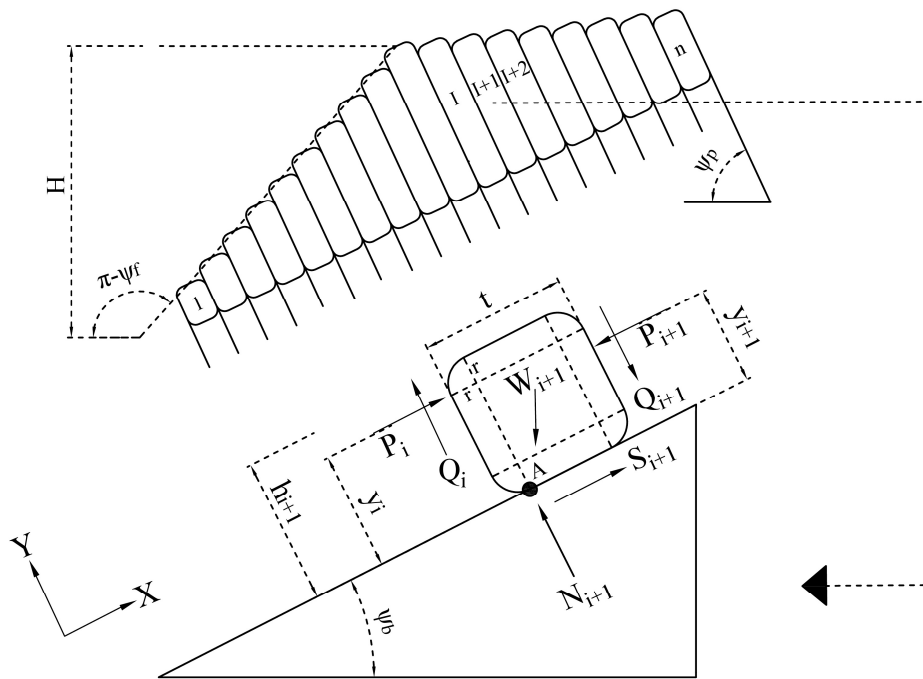


Figure 3. Schematic representation of the suggested theoretical solution.

$$Q_i = P_i \tan \varphi_{c,i} + C_{c,i} d_i \quad (11)$$

$$Q_{i+1} = P_{i+1} \tan \varphi_{c,i+1} + C_{c,i+1} d_{i+1} \quad (12)$$

$$y_{i+1} = h_{i+2} - r \quad (13)$$

$$y_i = h_{i+1} - r \quad (14)$$

As indicated in Figure 3, the application point of shear and normal forces at the base of the block is applied at point A, and the following supposition can be written:

$$S_{i+1} < (N_{i+1} \tan \phi_b + c_{b,i+1} t) \quad (15)$$

According to Figure 3, with regarding Equations (11, 12), the equation of moment equilibrium around point A can be obtained:

$$\begin{aligned} \sum M_A = 0 \rightarrow & 0.5W_{i+1}h_{i+1} \sin \psi_{b,i+1} - W_{i+1} \cos \psi_{b,i+1} (0.5t - r) + \\ & K_C W_{i+1} (\sin \psi_{b,i+1} (0.5t - r) + 0.5 \cos \psi_{b,i+1} h_{i+1}) + \\ & P_{i+1} y_{i+1} - (P_{i+1} \tan \varphi_{c,i+1} + C_{c,i+1} d_{i+1})(t - r) - P_i y_i - (P_i \tan \varphi_{c,i} + C_{c,i} d_i) r = 0 \end{aligned} \quad (16)$$

The magnitude of  $P_i$  can be computed as follows:

$$P_i = a_i + b_i P_{i+1} + c_i K_C \quad (17)$$

In the blocks of 1 and  $n$ , external forces are zero ( $P_{n+1} = P_0 = 0$ ). Hence, fictitious horizontal acceleration can be obtained as:

$$K_C = \frac{-[a_1 + a_2 b_1 + a_3 b_1 b_2 + \dots + a_n b_1 b_2 \dots b_{n-2} b_{n-1}]}{c_1 + c_2 b_1 + c_3 b_1 b_2 + \dots + c_n b_1 b_2 \dots b_{n-2} b_{n-1}} \quad (18)$$

in which:

$$a_i = \frac{[0.5W_{i+1} (h_{i+1} \sin \psi_{b,i+1} - \cos \psi_{b,i+1} (t - 2r)) - C_{c,i+1} d_{i+1} (t - r) - C_{c,i} d_i r]}{y_i + \tan \varphi_{c,i} r} \quad (19)$$

$$b_i = \frac{y_{i+1} - \tan \varphi_{c,i+1} (t - r)}{y_i + \tan \varphi_{c,i} r} \quad (20)$$

$$c_i = \frac{0.5W_{i+1} (h_{i+1} \cos \psi_{b,i+1} + \sin \psi_{b,i+1} (t - 2r))}{y_i + \tan \varphi_{c,i} r} \quad (21)$$

Computing the amount of the safety factor is the main purpose of the proposed approach. The flowchart for this obtaining this value is indicated in Figure 4. Firstly, the input parameters such as geometrical and mechanical specifications are set, and the safety factor is supposed to be equal to one. Next, using equations (18-21), the coefficients of  $a$ ,  $b$ ,  $c$ , and fictitious horizontal acceleration are calculated. Then regarding the sign of  $K_C$ , slope stability is specified. Finally, the safety factor is achieved with decreasing shear strength until  $K_C$  reaches zero.

#### 4. Assessment of Proposed Theoretical Approach

In this section, the suggested analytical method is evaluated with a typical example and standard case provided by Alejano and Alonso [32], as well as a case study.

##### 4.1. Typical example

Due to the time-consuming process of obtaining the safety factor, the suggested theoretical method was coded in a computer program to simplify the stability analysis of rock slopes with the potential of block toppling failure. The slope specification is given to the program, and the calculations related to the recommended approach are executed. A typical example, as shown in Figure 5, is examined with this code to assess the performance of the proposed theoretical solution.

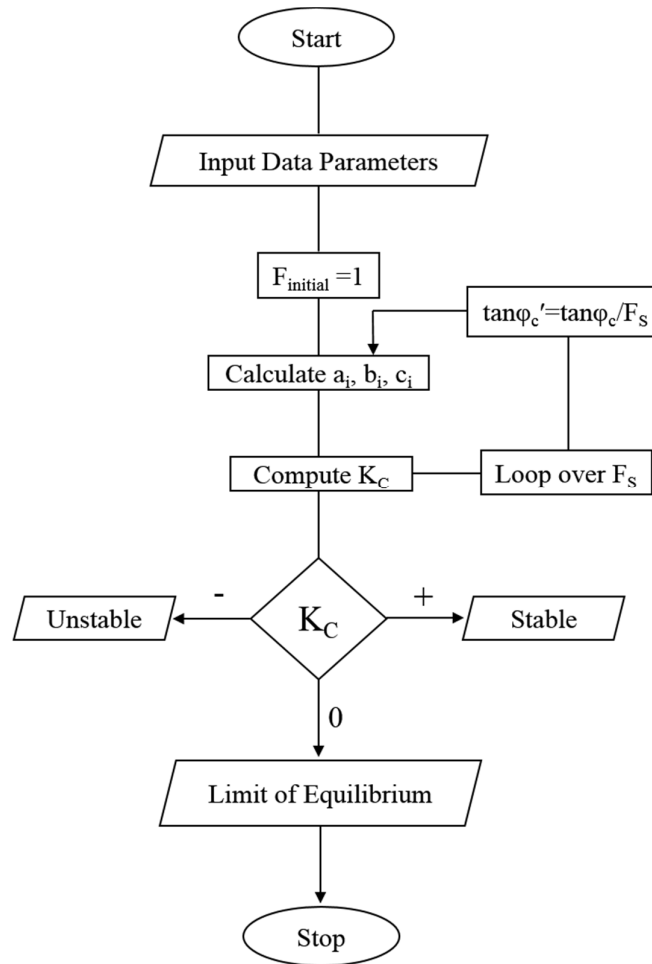


Figure 4. Flowchart for solving the proposed methodology.

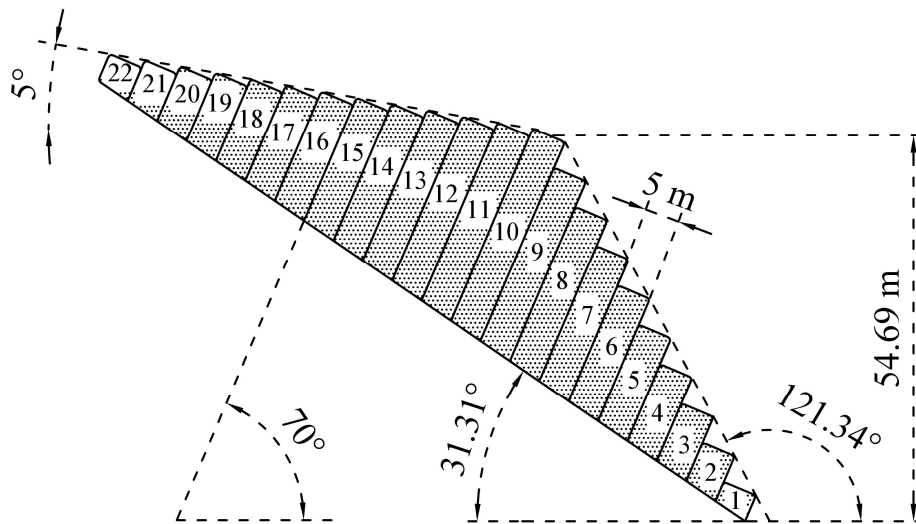


Figure 5. Schematic diagrams of a typical example.

The input parameters are listed at the top of Table 1, and the outcomes of this suggested approach and Goodman and Bray theory are listed in the bottom

portion. Additionally, the safety factor is shown in the bottom row of this table. The FS value obtained by the Goodman and Bray method is equal to

0.648. As shown in this table, in the suggested approach, the  $K_C$  value is computed to be  $2.9 \times 10^{-5}$ , nearly equal to zero, and the FS value is calculated at 0.682. This value is close to the corresponding value obtained by the Goodman and

Bray theory. The effect of various ratios of curvature radius to the block thickness ( $r/t = 0$  to 0.3) on the safety factor was also investigated. Figure 6 shows that the safety factor decreases non-linearly as block rounding increases.

**Table 1. Outcomes of stability analysis of typical example with the recommended theoretical and Goodman and Bray approaches.**

Properties							
Tensile strength (MPa)		Friction angle (Degree)		Friction angle between blocks (Degree)		Friction angle of base of blocks (Degree)	
3.5		35		30		35	
Column thickness (m)	Slope height (m)	Block number	Face slope angle (Degree)	Dip of basal plane (Degree)	Dip of blocks (Degree)	Dip of normal to discontinuities (Degree)	Dip of upper surface (Degree)
5	54.69	22	58.66	3131	70	20	5
Blocky toppling failure							
Goodman and Bray method (at $r/t = 0$ )				Proposed method (at $r/t = 0$ )			
Column number	Height (m)	Weight (kN)	Force (kN)	Failure mode	a	b	c
22	2.42	327.12	0.00	Stable	-261205.70	269127.22	-----
21	4.76	642.98	0.00	Stable	-207189.55	417535.37	-0.38
20	7.10	958.85	0.00	Stable	-153173.40	565943.52	0.07
19	9.44	1274.71	0.00	Stable	-99157.25	714351.67	0.30
18	11.78	1590.58	0.00	Stable	-45141.11	862759.82	0.44
17	14.12	1906.45	8.88	Toppling	8875.04	1011167.96	0.53
16	16.46	2222.31	69.49	Toppling	62891.19	1159576.11	0.60
15	18.80	2538.18	170.77	Toppling	116907.34	1307984.26	0.65
14	21.14	2854.04	307.56	Toppling	170923.49	1456392.41	0.69
13	23.48	3169.91	477.14	Toppling	224939.64	1604800.56	0.72
12	25.82	3485.77	677.99	Toppling	278955.79	1753208.71	0.75
11	28.16	3801.64	909.21	Toppling	332971.94	1901616.86	0.77
10	30.50	4117.50	1346.84	Toppling	339117.00	2067448.66	0.90
9	27.50	3712.50	1782.45	Toppling	263746.67	1879385.09	0.95
8	24.50	3307.50	2176.20	Toppling	186587.71	1691972.53	0.94
7	21.50	2902.50	2534.81	Toppling	106720.22	1505545.79	0.93
6	18.50	2497.50	2869.70	Toppling	22463.07	1320716.76	0.91
5	15.50	2092.50	3202.34	Toppling	-69619.14	1138735.82	0.89
4	12.50	1687.50	3579.75	Toppling	-177811.77	962618.59	0.85
3	9.50	1282.50	4135.35	Toppling	-328477.30	801960.23	0.78
2	6.50	877.50	5542.39	Toppling	-674518.08	712412.65	0.51
1	3.50	472.50	5291.79	Sliding	-270973.55	242290.26	-0.50
FS = 0.648						$K_C = 0.000029$	
						FS = 0.682	

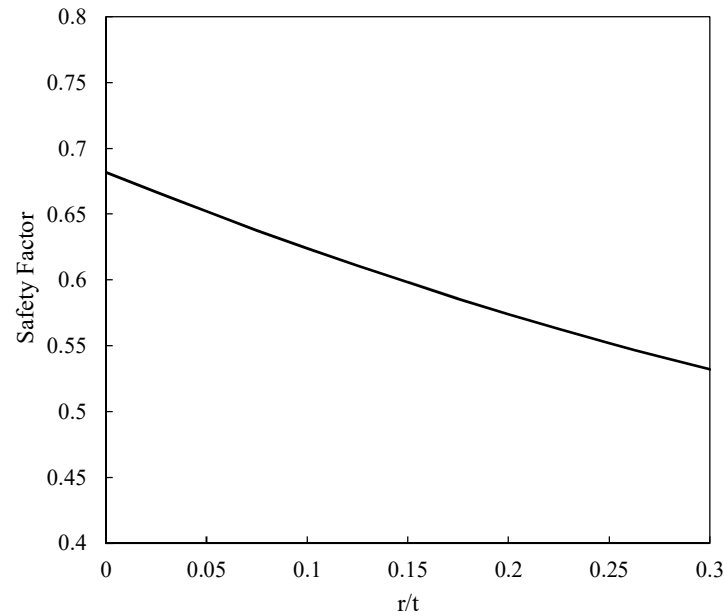


Figure 6. FS changes versus the ratio of curvature radius to block thickness in the typical example.

#### 4.2. A standard example of Alejano and Alonso

In this section, in standard examples presented by Alejano and Alonso [32], the changes in the safety factor against the curvature radii of edges, are investigated. Also the result of the proposed

analytical method is compared and verified with the analytical approach presented by Alejano *et al.* [29]. The input parameters are  $H = 10.95$  m,  $t = 1.75$  m,  $\gamma = 25$  kN/m<sup>3</sup>,  $\varphi_b = 30^\circ$ ,  $\varphi_c = 44^\circ$ . The schematic picture and other geometrical parameters are shown in Figure 7.

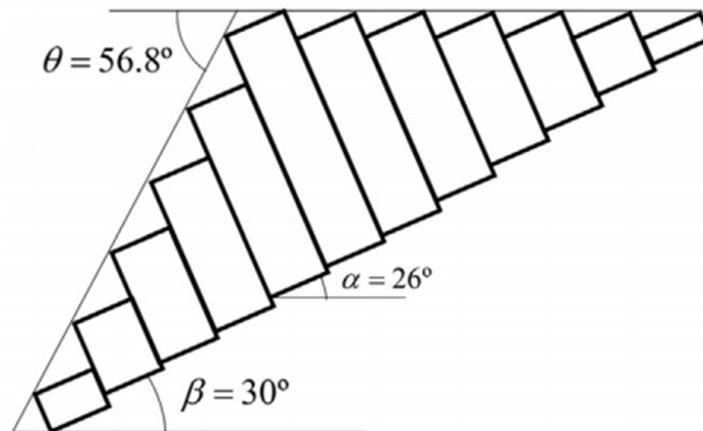


Figure 7. Geometrical parameters for example of Alejano and Alonso [32]

The results of the offered solution as well as Goodman and Bray method are given in Table 2 for sharp edges ( $r/t = 0$ ). For this case, the safety factors obtained by the proposed and Goodman and Bray approaches are 1.058 and 1.038, respectively. The factor of safety is calculated for different radii of curvature of the corners. These results are plotted in Figure 8. Also in this graph, the result

obtained from Alejano *et al.* [29] is plotted for comparison and validation with the proposed analytical method. As observed, by increasing the  $r/t$ , the safety factor drops below 0.85. It is concluded that edge rounding affects slope stability with a relatively small block number with the potential of toppling.

**Table 2. Result of the standard example provided by Alejano and Alonso [32].**

Column number	Goodman and Bray method (at $r/t = 0$ )				Proposed method (at $r/t = 0$ )		
	Height (m)	Weight (kN)	Force (kN)	Failure Mode	a	b	c
12	0.06	2.68	0.00	stable	-33818.95	17987.00	-----
11	0.98	42.97	0.00	Stable	-24988.91	36091.26	-1.55
10	1.90	83.25	0.00	Stable	-16158.87	54195.52	-0.32
9	2.82	123.54	0.00	Stable	-7328.84	72299.78	0.11
8	3.74	163.83	1.50	Toppling	1501.20	90404.04	0.33
7	4.67	204.11	11.03	Toppling	10331.24	108508.29	0.46
6	5.59	244.40	31.08	Toppling	23561.28	155686.59	0.68
5	4.67	204.11	38.84	Toppling	13306.43	139758.90	0.82
4	3.74	163.82	31.62	Toppling	2080.35	125315.43	0.76
3	2.82	123.54	9.13	Sliding	-11623.90	114658.99	0.63
2	1.90	83.25	0.00	Stable	-35769.97	119959.32	0.23
1	0.98	42.96	0.00	Stable	-24989.97	36089.08	-0.74
FS = 1.038					$K_C = 0.00035$		
					FS = 1.058		

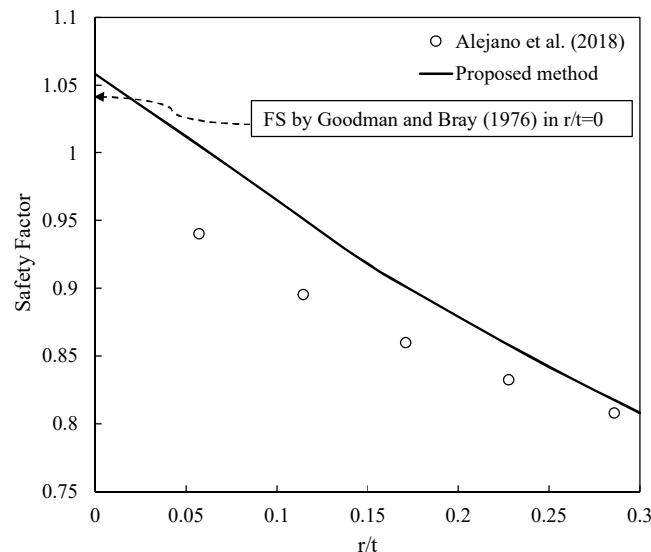


**Figure 8. FS variations versus the ratio of curvature radius to block thickness in standard example.**

**4.3. Case study**

The geological risk evaluation for slopes is the most significant of the studied mechanism. The role of this erosion-induced instability phenomenon is illustrated below, and the effect of weathering on block stability is quantified by investigating blocks with rounded edges subject to toppling mechanisms. In order to examine the effect of block edge rounding at field scale on

slopes, blocks from Monte Pindo, located in the municipality of Carnota, were analyzed. The rocks of this region are mainly biotite granite, pink in color, with medium to fine sand [29]. The Monte Pindo region has many weathered boulders with the potential of toppling. This case study referred to five blocks that are stable because the last block prevented the upstream blocks from toppling (as shown in Figure 9).

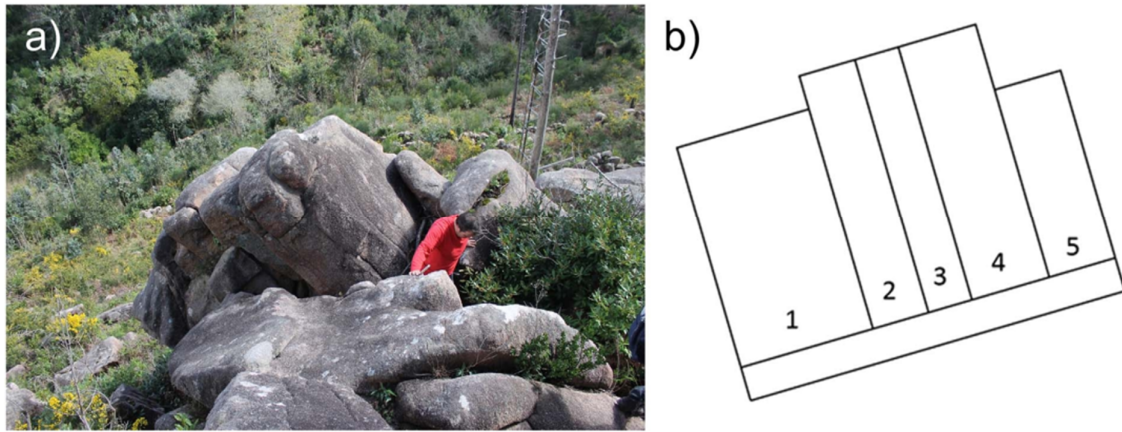


Figure 9. Case study, a) site picture, b) cross-section view [29].

The geometry is summarized in Table 3 by Alejano *et al.* [29]. The geomaterial parameters are  $\gamma = 25.5 \text{ kN/m}^3$ ,  $\phi_b = 35^\circ$ ,  $\phi_c = 30^\circ$ ,  $\psi_b = 10^\circ$ . The safety factor for blocks with sharp edges was found to be 3.27 using the Goodman and Bray method. Furthermore, Alejano *et al.* [29] obtained a safety factor for blocks with rounded edge blocks equal to 0.91. In the proposed theoretical solution, the value of the safety factor for the sharp-edged and rounded-edged blocks are obtained at 3.59 and 0.952, respectively (as shown in Figure 10). The results show that the suggested analytical approach has an acceptable accuracy with the results

corresponding to the existing analytical methods. Considering weathering, the safety factor is on the threshold of instability.

Table 3. Case study measurements [29].

Block	h (m)	t (m)	r (m)
5	1.7	0.6	0.25
4	2.3	0.7	0.25
3	2.3	0.4	0.2
2	2.3	0.5	0.25
1	2	1.2	0.25

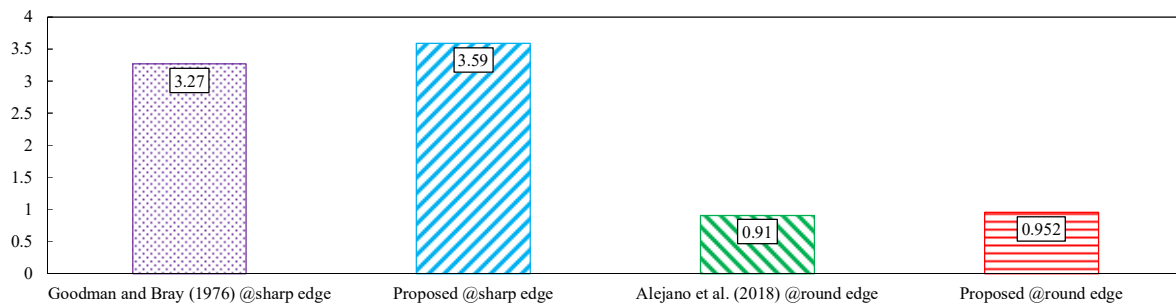


Figure 10. Comparison of safety factors in sharp and rounded edges in the case study.

### 5. Conclusions

A particular characteristic of spheroidal weathering is the rounding of block edges. In this work, applying the Sarma methodology, a new analytical approach was offered for stability analysis of block toppling failure regarding the erosion phenomenon. The advantage of the suggested method is that it is a simple solution to evaluate slope stability. In this regard, by computing the coefficients a, b, c, and  $K_C$ , the slope stability is specified. Due to the time-consuming manual calculation of the stability analysis in the

proposed theoretical approach, a program code was created in Excel for simplifying the stability analysis of the mentioned failure. The proposed analytical solution was compared and verified by using two typical and standard examples as well as a case study with the pre-existing theoretical methods of Goodman and Bray (1976) and Alejano *et al.* (2018), which were for sharp and rounded edges, respectively, and acceptable results were obtained. It could be concluded that with the weathering; the safety factor decreased in a non-linear way. This effect of reducing the safety factor was greater for thick blocks. This proposed

theoretical solution is suitable to assess the toppling instability of rounded blocks.

### Acknowledgments

The authors wish to express their scientific thanks to Professor Ömer Aydan and Dr. Mehdi Amini for their invaluable guidance through this research work.

### References

- [1]. Müller, L. (1968). New considerations on the Vaiont slide, *Rock Mech Eng Geol.*, 6: 1–91.
- [2]. Erguvanli, R. and Goodman, K. (1970). Applications of models to engineering geology for rock excavations, *Assoc Eng Geol.*, 9.
- [3]. Ashby, J. (1971). Sliding and toppling modes of failure in models and jointed rock slopes, Imperial College, University of London.
- [4]. Wyllie, D.C., Mah, C.W., and Hoek, E. (2004). *Rock Slope Engineering : civil and mining*. Spon Press.
- [5]. Sarfaraz, H. and Amini, M. (2020). Numerical Simulation of Slide-Toe-Toppling Failure using Distinct Element Method and Finite Element Method, *Geotech. Geol. Eng.*, 38 (2): 2199–2212.
- [6]. Sarfaraz, H. (2020). A simple theoretical approach for analysis of slide-toe-toppling failure, *J. Cent. South Univ.*, 27 (9).
- [7]. Sarfaraz, H., Bahrami, A.R., and Samani, R. (2022). Numerical Modelling of Slide-Head-Toppling Failure using FEM and DEM Methods, *J. Min. Environ.*, 13 (1): 269–280.
- [8]. Sari, M. (2021). Secondary toppling failure analysis and optimal support design for ignimbrites in the Ihlara Valley (Cappadocia, Turkey) by finite element method (FEM), *Geotech. Geol. Eng.*, 39 (7): 5135–5160.
- [9]. Aydan, Ö. and Kawamoto, T. (1987). Toppling failure of discontinuous rock slopes and their stabilization (in Japanese), *J. Japan Min. Soc.*, 103: 763–770.
- [10]. Aydan, Ö. and Kawamoto, T. (1992). The stability of slopes and underground openings against flexural toppling and their stabilisation, *Rock Mech. Rock Eng.*, 25 (3):143–165.
- [11]. Pritchard, M.A. and Savigny, K.W. (1991). The Heather Hill landslide: an example of a large scale toppling failure in a natural slope, *Can. Geotech. J.*, 28: 410–422.
- [12]. Alzo`ubi, A.K., Martin, C.D., and Cruden, D.M. (2010). Influence of tensile strength on toppling failure in centrifuge tests, *Int. J. Rock Mech. Min. Sci.*, 47 (6): 974–982.
- [13]. Amini, M., Majdi, A., and Aydan, Ö. (2009). Stability analysis and the stabilization of flexural toppling failure, *Rock Mech. Rock Eng.*, 42 (5):751–782.
- [14]. Majdi, A. and Amini, M. (2011). Analysis of geo-structural defects in flexural toppling failure, *Int. J. Rock Mech. Min. Sci.*, 48 (2):175–186.
- [15]. Amini, M., Majdi, A., and Veshadi, M.A. (2012). Stability analysis of rock slopes against block-flexure toppling failure, *Rock Mech. Rock Eng.*, 45 (4): 519–532.
- [16]. Sarfaraz, H. (2020). Stability Analysis of Flexural Toppling Failure using the Sarma's Method, *Geotech. Geol. Eng.*, 38 (4): 3667–3682.
- [17]. Sarfaraz, H. (2020). Stability analysis of block-flexural toppling of rock blocks with round edges, *J. Min. Environ.*, 11(4):1217–1229.
- [18]. Bowa, V.M. and Xia, Y. (2019). Influence of counter-tilted failure surface angle on the stability of rock slopes subjected to block toppling failure mechanisms, *Bull. Eng. Geol. Environ.*, 78 (4): 2535–2550.
- [19]. Sarfaraz, H. and Amini, M. (2020). Numerical Modeling of Rock Slopes with a Potential of Block-Flexural Toppling Failure, *J. Min. Environ.*, 11(1): 247–259.
- [20]. Zheng, Y., Chen, C., Liu, T., Zhang, H., and Sun, C. (2019). Theoretical and numerical study on the block-flexure toppling failure of rock slopes, *Eng. Geol.*, 263:105309.
- [21]. Zheng, Y., Chen, C., Meng, F., Zhang, H., Xia, K., and Chen, X. (2020). Assessing the stability of rock slopes with respect to block-flexure toppling failure using a force-transfer model and genetic algorithm, *Rock Mech. Rock Eng.*, 53 (8): 3433–3445.
- [22]. Yaylaci, M. (2022). Simulate of edge and an internal crack problem and estimation of stress intensity factor through finite element method, *Adv. nano Res.*, 12 (4): 405-414.
- [23]. Öner, E., Sengül, B., Sabano, C., Yaylaci, E., Adiyaman, G., Yaylaci, M., and Birinci, A. (2022). On the plane receding contact between two functionally graded layers using computational, finite element and artificial neural network methods, *ZAMM-Journal Appl. Math. Mech. für Angew. Math. und Mech.*, 102 (2): 202100287.
- [24]. Turan, M., Yaylaci, M., and Yaylaci, M. (2022). Free vibration and buckling of functionally graded porous beams using analytical, finite element, and artificial neural network methods, *Arch. Appl. Mech.*, 1–22.
- [25]. Yaylaci, E., Oner, E., Yaylaci, M., Ozdemir, M., Abushattal, A., and Birinci, A. (2022). Application of

artificial neural networks in the analysis of the continuous contact problem, *Struct. Eng. Mech.*, 84 (1).

[26]. Yaylaci, M., Abanoz, M., Yaylaci, E., Ölmez, H., Sekban, D., and Birinci, A. (2022). The contact problem of the functionally graded layer resting on rigid foundation pressed via rigid punch” *Steel Compos. Struct.*, 43 (5).

[27]. Yaylaci, M., Sabano, B.S., Ozdemir, M.E., and Birinci, A. (2022). Solving the contact problem of functionally graded layers resting on a HP and pressed with a uniformly distributed load by analytical and numerical methods, *Struct. Eng. Mech.*, 82 (3): 401–416.

[28]. Alejano, L. R., Carranza-Torres, C., Giani, G. P., and Arzúa, J. (2015). Study of the stability against toppling of rock blocks with rounded edges based on

analytical and experimental approaches, *Eng. Geol.*, 195: 172–184.

[29]. Alejano, L.R. et al. (2018). Block toppling stability in the case of rock blocks with rounded edges, *Eng. Geol.*, 234: 192–203.

[30]. Sarma, S.K. (1979). Stability analysis of embankments and slopes, *J. Geotech. Geoenvironmental Eng.*, 105:15068.

[31]. Goodman, R.E. and Bray, J.W. (1976). Toppling of rock slopes In: *Rock engineering for foundations and slopes*, Am. Soc. Civ. Eng., New York.

[32]. Alejano, L.R. and Alonso, E. (2005). Application of the shear and tensile strength reduction technique to obtain factors of safety of toppling and footwall rock slopes, in *ISRM International Symposium-EUROCK 2005*.

## تحلیل پایداری شکست واژگونی بلوکی با بلوکهای گرد شده با استفاده از روش سارما

حسن سرفراز<sup>\*</sup>، محدثه سرلک، فاطمه عاشور و عرفان امینی

دانشکده مهندسی معدن، دانشگاه تهران، تهران، ایران

ارسال ۲۰۲۳/۰۱/۲۳، پذیرش ۲۰۲۳/۰۳/۰۳

\* نویسنده مسئول مکاتبات: sarfaraz@ut.ac.ir

---

### چکیده:

شکست واژگونی بلوکی یکی از ناپایداری‌های رایج شیروانی‌های سنگی است. در این ناپایداری، توده سنگ از یک سری ناپیوستگی‌های موازی و درزه‌های متقاطع نسبت به این ناپیوستگی‌ها تشکیل شده است. بلوک‌ها ممکن است به دلیل وزنشان در راستای درزه‌های متقاطع بلغزند یا واژگون شوند. مقاومت کششی تأثیر قابل توجهی بر پایداری شکست واژگونی بلوکی ندارد. گردشگری لبه‌های ستون سنگی از ویژگی‌های خاص هوازدهی است. ابتداء مروری بر ادبیات ش واژگونی بلوکی ارائه شده است. سپس با استفاده از روش سارما، یک روش تحلیل پایداری جدید برای ستون‌های سنگی با لبه‌های گرد پیشنهاد شده است. یکی از مزایای روش پیشنهادی این است که با تعیین علامت پارامتری به نام Kc می‌توان وضعیت پایداری را تعیین نمود. روش تحلیلی پیشنهادی با یک روش تنوری از طریق مثال‌ها و مطالعه موردی مقایسه شده است. مقایسه نتایج نشان می‌دهد که روش تحلیلی پیشنهادی تطابق قابل قبولی دارد. می‌توان نتیجه گرفت که با هوازدهی و گردش لبه‌های بلوک، فاکتور ایمنی به صورت غیرخطی کاهش می‌یابد. از روش تحلیلی ارائه شده می‌توان برای ارزیابی شکست واژگونی بلوکی با در نظر گرفتن پدیده فرسایش استفاده کرد.

**کلمات کلیدی:** شیروانی‌های سنگی، واژگونی بلوکی، روش تحلیلی، روش سارما، تعادل حدی، فاکتور ایمنی.

---